Angewandte Chemie
Eine Zeitschrift der Gesellschaft Deutscher Chemiker

Supporting Information

69451 Weinheim, Germany

Triphenylamine-Dendronized Pure Red Iridium Phosphors with Superior OLED Efficiency/Color Purity Trade-offs

Guijiang Zhou, Wai-Yeung Wong, Bing Yao, Zhiyuan Xie* and Lixiang Wang*

Experimental

General Information: All reactions were performed under nitrogen atmosphere. Solvents were carefully dried and distilled from appropriate drying agents prior to use. Commercially available reagents were used without further purification unless otherwise stated. All reactions were monitored by thin-layer chromatography (TLC) with Merck pre-coated glass plates. Flash column chromatography and preparative TLC were carried out using silica gel from Merck (230-400 mesh). Fast atom bombardment (FAB) mass spectra were recorded on a Finnigan MAT SSQ710 system. Proton NMR spectra were measured in $CDCl_3$ on a Varian Inova 400 MHz FT-NMR spectrometer; chemical shifts were quoted relative to tetramethylsilane.

Physical Measurements: UV–vis spectra were obtained on a HP-8453 spectrophotometer. The photoluminescent properties and lifetimes of the compounds were probed on the Photon Technology International (PTI) Fluorescence Master Series QM1 system. The phosphorescence quantum yields were determined in CH_2Cl_2 solutions at 293 K against *fac*-[$Ir(ppy)_3$] standard (Φ_P = 0.40).[12] For solid-state emission spectral measurements, the 325 nm line of a He–Cd laser was used as an excitation source. The luminescence spectra were analyzed by a 0.25 m focal length double monochromator with a Peltier cooled photomultiplier tube and processed with a lock-in-amplifier. Electrochemical measurements were made using a Princeton Applied Research model 273A potentiostat at a scan rate of 100 mV s^{-1}. A conventional three-electrode configuration consisting of a platinum or glassy carbon working electrode, a Pt-wire counter electrode, and an Ag/AgCl reference electrode was used. The supporting electrolyte was 0.1 M $[Bu_4N]PF_6$. For the anodic scan, the potentials were measured in CH_2Cl_2 solution using a platinum working electrode whereas for the cathodic scan, the measurements were done in THF solution with a glass carbon working electrode. Ferrocene was added as a calibrant after each set

of measurements, and all potentials reported were quoted with reference to the ferrocene-ferrocenium (Fc/Fc^+) couple. Thermal analyses were performed with the Perkin-Elmer Pyris Diamond DSC and Perkin-Elmer TGA6 thermal analyzers.

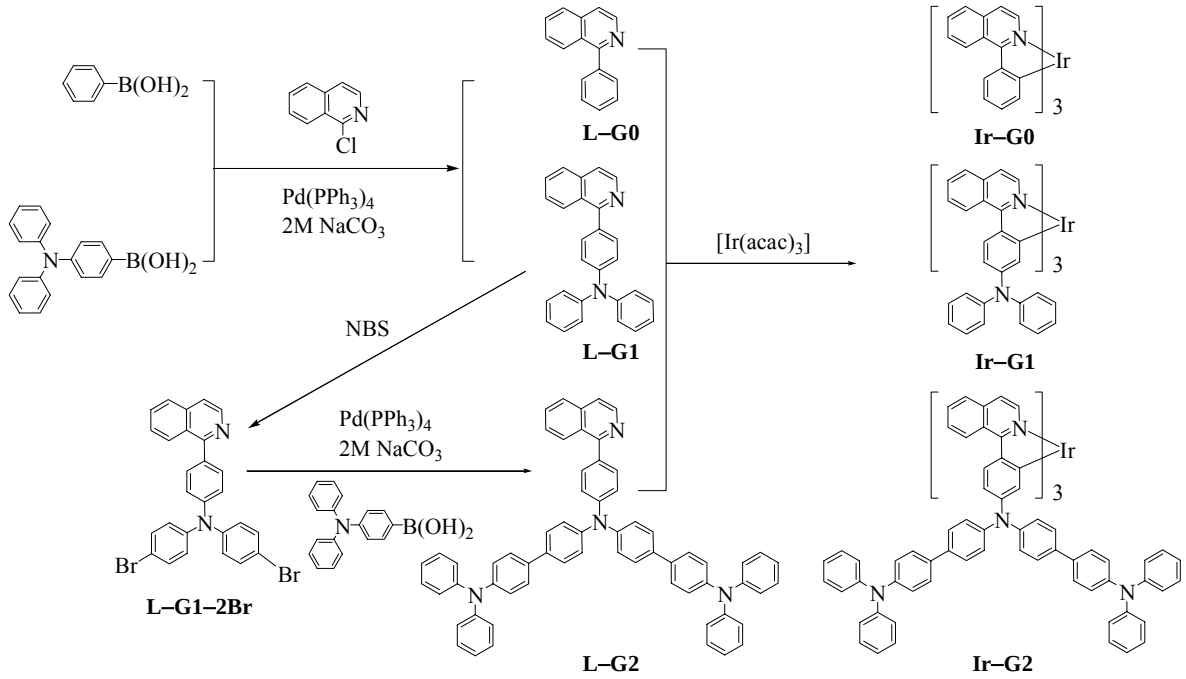

Scheme 1

L–G0, **Ir–G0** and *N*,*N*'-diphenyl-4-aminophenylboronic acid were synthesized following the literature methods.[11,13]

Synthesis of ***L–G1***. Under N_2 atmosphere, 1-chloro-isoquinoline (0.50 g, 3.06 mmol), 4-diphenylaminophenylboronic acid (0.97 g, 3.36 mmol) and $Pd(PPh_3)_4$ (177 mg) were added to a mixture of toluene (30 mL) and 2M Na_2CO_3 (20 mL). The reaction mixture was heated to 110 ^oC for 48 h under stirring. Then the reaction mixture was cooled to room temperature and extracted with CH_2Cl_2 (3 × 50 mL). The combined organic phase was washed with water (3 × 100 mL). The organic phase was separated and dried over $MgSO_4$. The solvent was removed under reduced pressure and the residue was purified by column chromatography eluting with CH_2Cl_2. The product was obtained as a white crystalline solid (1.04 g, 91%). ^1H NMR ($CDCl_3$):

δ (ppm) 8.59 (d, J = 5.6 Hz, 1H, Ar), 8.23 (d, J = 8.4 Hz, 1H, Ar), 7.87 (d, J = 8.4 Hz, 1H, Ar), 7.72–7.68 (m, 1H, Ar), 7.63–7.55 (m, 4H, Ar), 7.32–7.18 (m, 10H, Ar), 7.09–7.04 (m, 2H, Ar). ^{13}C NMR ($CDCl_3$): δ (ppm) 160.23, 148.29, 147.45, 142.13, 136.88, 133.14, 130.88, 129.34, 129.27, 127.60, 127.03, 126.95, 126.55, 124.67, 123.15, 122.89, 119.52 (Ar). FAB-MS (*m/z*): 372 $[M+1]^+$. Anal. calcd. for $C_{27}H_{20}N_2$: C, 87.07; H, 5.41; N, 7.52; found: C, 86.88; H, 5.32; N, 7.40.

Synthesis of ***L–G1–2Br***. **L–G1** (0.60 g, 1.61 mmol) and NBS (0.59 g, 3.30 mmol) were added to chloroform (30 mL) under N_2 atmosphere and several drops of acetic acid were then added. The mixture was stirred at room temperature for an hour and then heated to gentle reflux overnight. Then it was cooled to room temperature and water (100 mL) was added. The mixture was extracted with CH_2Cl_2 (3 × 50 mL). The combined organic phase was dried over $MgSO_4$. The solvent was removed under reduced pressure and the residue was purified by column chromatography with chloroform as the eluent. The product was obtained as a white crystalline solid (0.81 g, 95%). ^{1}H NMR ($CDCl_3$): δ (ppm) 8.59 (d, J = 5.6 Hz, 1H, Ar), 8.18 (dd, J = 0.8, 8.4 Hz, 1H, Ar), 7.88 (d, J = 8.4 Hz, 1H, Ar), 7.72–7.68 (m, 1H, Ar), 7.64–7.55 (m, 4H, Ar), 7.41–7.37 (m, 4H, Ar), 7.22–7.19 (m, 2H, Ar), 7.06–7.03 (m, 4H, Ar). ^{13}C NMR ($CDCl_3$): δ (ppm) 159.93, 147.34, 146.23, 142.23, 136.93, 134.47, 132.46, 131.20, 130.02, 127.41, 127.16, 127.06, 126.54, 125.90, 123.57, 119.75, 115.98 (Ar). FAB-MS (*m/z*): 530 $[M]^+$. Anal. calcd. for $C_{27}H_{18}Br_2N_2$: C, 61.16; H, 3.42; N, 5.28; found: C, 61.02; H, 3.33; N, 5.35.

Synthesis of ***L–G2***. **L–G1–2Br** (0.60 g, 1.13 mmol), 4-diphenylaminophenylboronic acid (0.72 g, 2.49 mmol) and $Pd(PPh_3)_4$ (65 mg) were added to a mixture of toluene (30 mL) and 2M Na_2CO_3 (20 mL) under nitrogen. The reaction mixture was heated to 110 ^{o}C for 24 h under stirring. After cooling to room temperature, 4-diphenylaminophenylboronic acid (0.36 g, 1.25

mmol) and $Pd(PPh_3)_4$ (65 mg) were added to the reaction flask again. The reaction was allowed to proceed at 110 ^oC for another 24 h. Then the reaction mixture was cooled to room temperature and extracted with CH_2Cl_2 (3 × 60 mL). The combined organic phase was washed with water (3 × 150 mL). The organic phase was separated and dried over $MgSO_4$. The solvent was removed under reduced pressure and the residue was purified by column chromatography with CH_2Cl_2 as eluent. The product was obtained as a pale yellow solid (0.86 g, 89 %). ^1H NMR ($CDCl_3$): δ (ppm) 8.60 (d, J = 6.0 Hz, 1H, Ar), 8.25 (d, J = 8.8 Hz, 1H, Ar), 7.88 (d, J = 8.4 Hz, 1H, Ar), 7.72–7.68 (m, 1H, Ar), 7.67–7.56 (m, 4H, Ar), 7.54–7.46 (m, 8H, Ar), 7.32–7.25 (m, 14H, Ar), 7.15–7.13 (m, 12H, Ar), 7.05–7.01 (m, 4H, Ar). ^{13}C NMR ($CDCl_3$): δ (ppm) 160.22, 148.03, 147.63, 146.78, 146.20, 142.23, 136.90, 135.36, 134.52, 133.55, 131.01, 129.92, 129.21, 127.58, 127.41, 127.31, 127.05, 126.98, 126.57, 124.76, 124.28, 123.99, 123.25, 122.80, 119.53 (Ar). FAB-MS (*m/z*): 859 $[M]^+$. Anal. calcd. for $C_{63}H_{46}N_4$: C, 88.08; H, 5.40; N, 6.52; found: C, 87.86; H, 5.22; N, 6.50.

Synthesis of ***Ir–G1***. Under a nitrogen flow, **L–G1** (0.50 g, 1.34 mmol) and $[Ir(acac)_3]$ (0.19 g, 0.39 mmol) were added to glycerol (18 mL). Then the reaction mixture was heated at 230 ^oC for 24 h. After cooling to room temperature, the reaction mixture was poured into water (150 mL) and extracted with CH_2Cl_2 (3 × 60 mL). The organic phase was separated and dried over $MgSO_4$. Then the solvent was removed under reduced pressure and the residue was purified by column chromatography with CH_2Cl_2/hexane (3:1) as eluent. The product was obtained as a dark red solid (0.15 g, 30%). ^1H NMR ($CDCl_3$): δ (ppm) 8.81 (d, J = 9.2 Hz, 3H, Ar), 7.80 (d, J = 8.6 Hz, 3H, Ar), 7.72–7.58 (m, 9H, Ar), 7.35 (d, J = 6.2 Hz, 3H, Ar), 7.08–6.76 (m, 36H, Ar), 6.28–6.23 (dd, J_1 = 2.4, 8.9 Hz, 3H, Ar). ^{13}C NMR ($CDCl_3$): δ (ppm) 166.43, 165.98, 147.96, 147.31, 140.07, 138.67, 136.47, 132.23, 130.67, 129.65, 129.29, 128.52, 127.58, 126.73, 126.00,

124.98, 122.33, 118.61, 114.10 (Ar). FAB-MS (*m/z*): 1307 $[M+1]^+$. Anal. calcd. for $C_{81}H_{57}IrN_6$: C, 74.46; H, 4.40; N, 6.43; found: C, 74.23; H, 4.25; N, 6.29.

Synthesis of ***Ir–G2***. This compound was prepared following analogous procedures as for **Ir-G1**, and **Ir–G2** was obtained as an orange-red solid in 12% yield. ^{1}H NMR ($CDCl_3$): δ (ppm) 8.86 (d, J = 8.8 Hz, 3H, Ar), 7.90 (d, J = 8.8 Hz, 3H, Ar), 7.73 (d, J = 8.0 Hz, 3H, Ar), 7.64–7.54 (m, 6H, Ar), 7.36 (d, J = 5.6 Hz, 3H, Ar), 7.28–7.26 (m, 15H, Ar), 7.22–7.16 (m, 36H, Ar), 7.08–6.94 (m, 54H, Ar), 6.83 (d, J = 8.8 Hz, 12H, Ar), 6.41–6.38 (dd, J = 2.4, 8.8 Hz, 3H, Ar). ^{13}C NMR ($CDCl_3$): δ (ppm) 166.56, 166.16, 147.87, 147.71, 146.37, 146.11, 140.10, 139.41, 136.59, 134.87, 134.07, 130.74, 130.60, 129.86, 129.19, 127.58, 127.15, 126.99, 126.93, 126.73, 126.15, 124.64, 124.20, 124.04, 122.61, 118.98, 115.01 (Ar). FAB-MS (*m/z*): 2766 $[M]^+$. Anal. calcd. for $C_{189}H_{135}IrN_{12}$: C, 82.06; H, 4.92; N, 6.08; found: C, 81.92; H, 4.76; N, 5.86.

OLED Fabrication and Measurements: The pre-cleaned ITO glass substrates were treated by ozone for 20 min. Then 50 nm thick PEDOT:PSS film was first deposited on the ITO glass substrates, and cured at 120 °C for 30 min in air. The emitting layer was obtained by spin-coating a chloroform solution of the dendrimer at a concentration of 8 mg mL^{-1}. Successively, BCP, Alq_3, LiF and Al were evaporated at a base pressure less than 10^{-6} torr. The EL spectra and CIE coordinates were measured with a PR650 spectra colorimeter. The *L–V–J* curves of the devices were recorded by a Keithley 2400/2000 source meter and a calibrated silicon photodiode. All the experiments and measurements were carried out at room temperature under ambient conditions.

References:

[12] K. A. King, P. J. Spellane, R.-J. Watts, *J. Am. Chem. Soc.* **1985**, *107*, 1431.

[13] R. Pudzich, J. Salbeck, *Synth. Met.* **2003**, *138*, 21.

Table S1: Photophysical and thermal data for the iridium dendrimers.

Compound	Absorption (298 K) λ_{abs} [nm] [a]	Emission (298 K) λ_{em} [nm] CH_2Cl_2/film	Φ_p [b]	τ_p [μs] [c]	$\Delta T_{5\%}/T_g$ [^oC] [d]	HOMO/LUMO [eV]
Ir–G0	320 (3.35), 425 (3.02), 469 (2.86), 540 (2.21)	620/628	0.28	0.81	417/145	–5.11/–2.44
Ir–G1	300 (3.65), 422 (3.53), 448 (3.51), 520 (2.84)	636/646	0.13	1.21	433/162	–4.99/–2.34
Ir–G2	312 (4.14), 376 (4.18), 436 (3.73), 461 (3.75), 530 (3.04)	641/643	0.12	1.40	460/220	–4.96/–2.38

[a] Measured in CH_2Cl_2 at a concentration of 10^{-5} M and logε values are shown in parentheses. [b] In degassed CH_2Cl_2 relative to *fac*-[Ir(ppy)$_3$] (Φ_p = 0.4), λ_{ex} = 410 nm. [c] Measured in toluene at a concentration of 10^{-5} M for the sample solution, the excitation wavelength was set at 337 nm for all the samples at 298 K. [d] $\Delta T_{5\%}$ is the 5% weight-reduction temperature and T_g is the glass transition temperature.

Table S2: Performance of Ir^{III} dendrimer doped electrophosphorescent OLEDs.

Device	Phosphor dopant	$V_{turn\text{-}on}$ [V]	Luminance L [cd m^{-2}]	η_{ext} [%]	η_L [cd A^{-1}]	η_p [lm W^{-1}]	λ_{max} [nm] [d]
A	**Ir–G1** (8 wt.-%)	4.4	7451 (17) [a]	11.65 (5) [a]	5.82 (5)	3.65 (5)	640
				7.01 [b]	3.49	1.36	(0.70, 0.30)
				4.85 [c]	2.42	0.61	
B	**Ir–G1** (10 wt.-%)	4.3	6239 (18) [a]	10.25 (5) [a]	5.07 (5)	3.18 (5)	640
				6.68 [b]	3.31	1.18	(0.70, 0.30)
				4.53 [c]	2.24	0.51	
C	**Ir–G1** (12 wt.-%)	4.0	5890 (17) [a]	5.43 (6) [a]	2.83 (6)	1.77 (5)	640
				4.45 [b]	2.37	0.89	(0.70, 0.30)
				3.25 [c]	1.69	0.44	
D	**Ir–G2** (8 wt.-%)	4.7	6162 (16) [a]	4.58 (9) [a]	2.35 (9)	0.90 (8)	640
				4.57 [b]	2.34	0.84	(0.70, 0.30)
				3.78 [c]	1.93	0.50	
E	**Ir–G2** (10 wt.-%)	4.7	6143(16) [a]	7.36 (6) [a]	3.72 (6)	2.29 (5)	640
				5.31 [b]	2.68	0.95	(0.70, 0.30)
				3.85 [c]	1.94	0.47	
F	**Ir–G2** (12 wt.-%)	4.7	6205 (17) [a]	6.42 (7) [a]	3.18 (7)	2.08 (7)	640
				4.68 [b]	2.31	0.84	(0.70, 0.30)
				3.43 [c]	1.69	0.41	

[a] Maximum values of the devices. Values in parentheses are the voltages at which they were obtained. [b] Values collected at 100 cd m^{-2}. [c] Values collected at 1000 cd m^{-2}. [d] CIE coordinates [x, y] in parentheses.

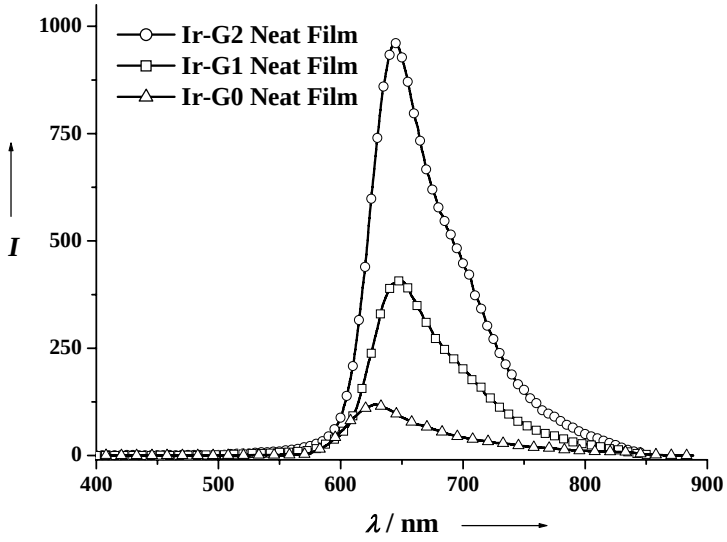

Figure S1. The PL spectra for the neat films of iridium dendritic complexes at 290 K.

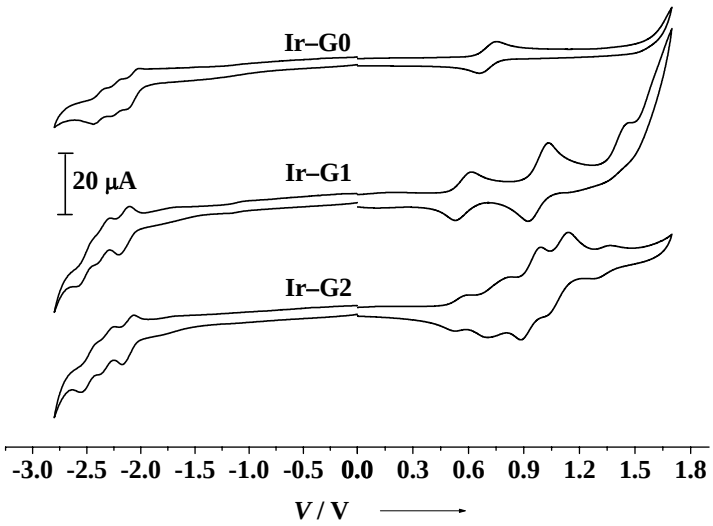

Figure S2. Cyclic voltammograms for the iridium dendrimers.

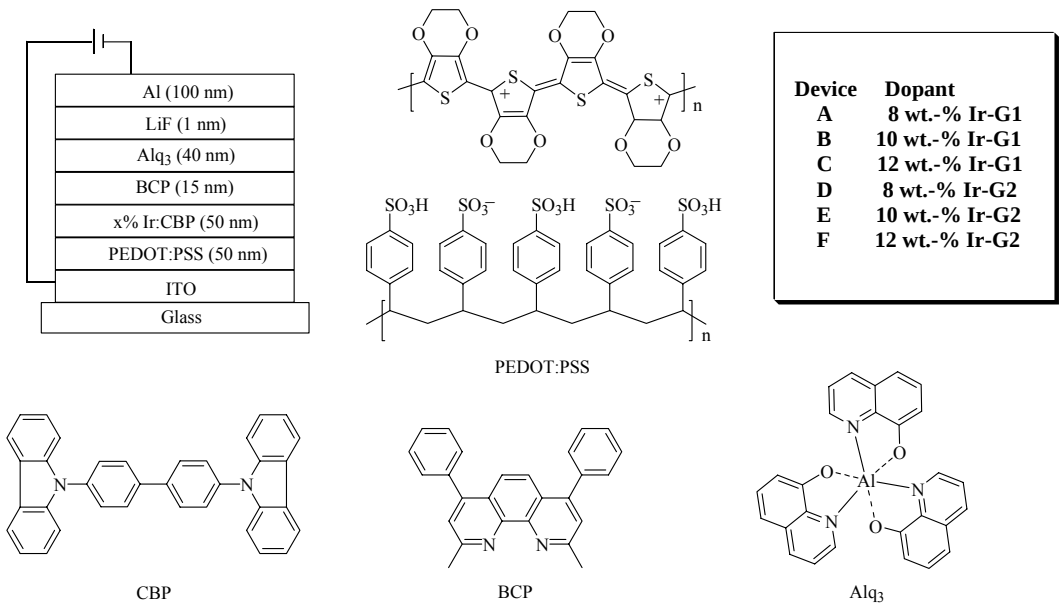

Figure S3. The general configuration for OLED devices and the molecular structures of the relevant compounds used in these devices.

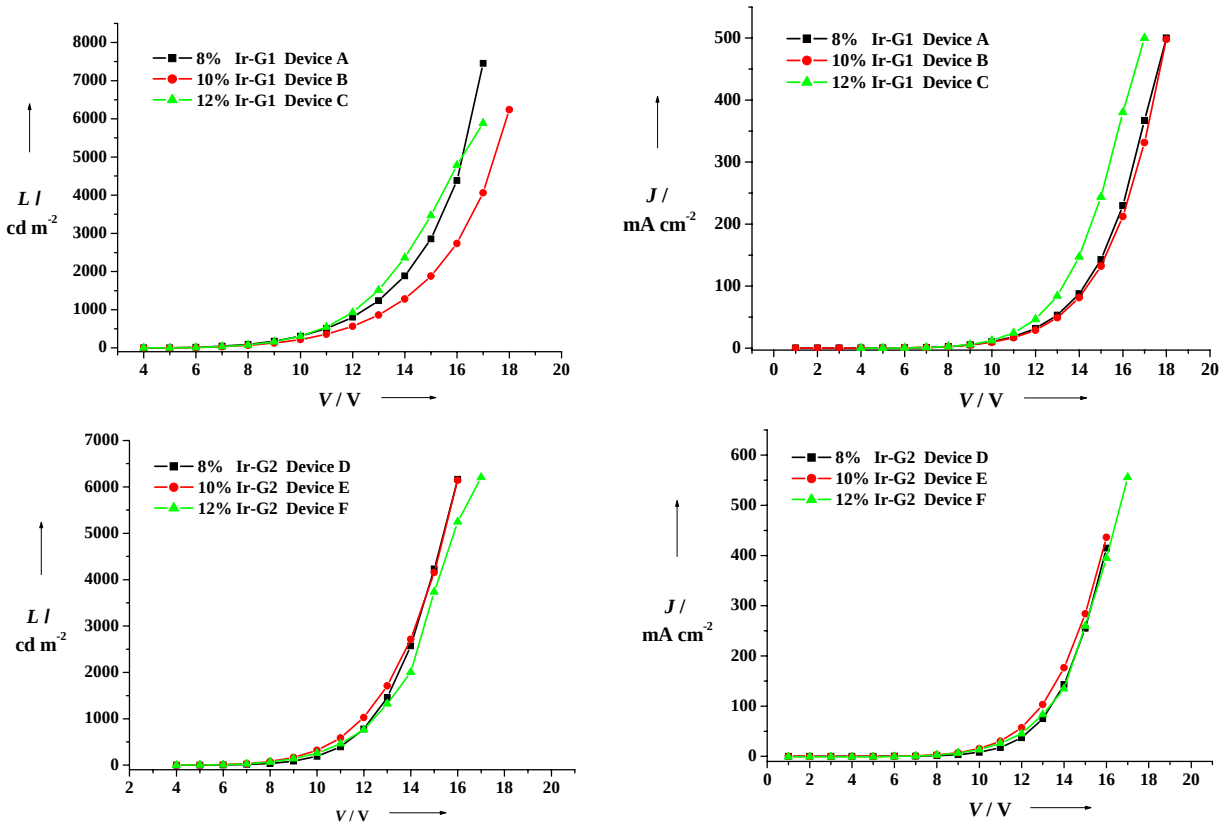

Figure S4. The luminance–voltage–current density (*L*–*V*–*J*) characteristics of devices with different doping levels of **Ir–G1** and **Ir–G2**.

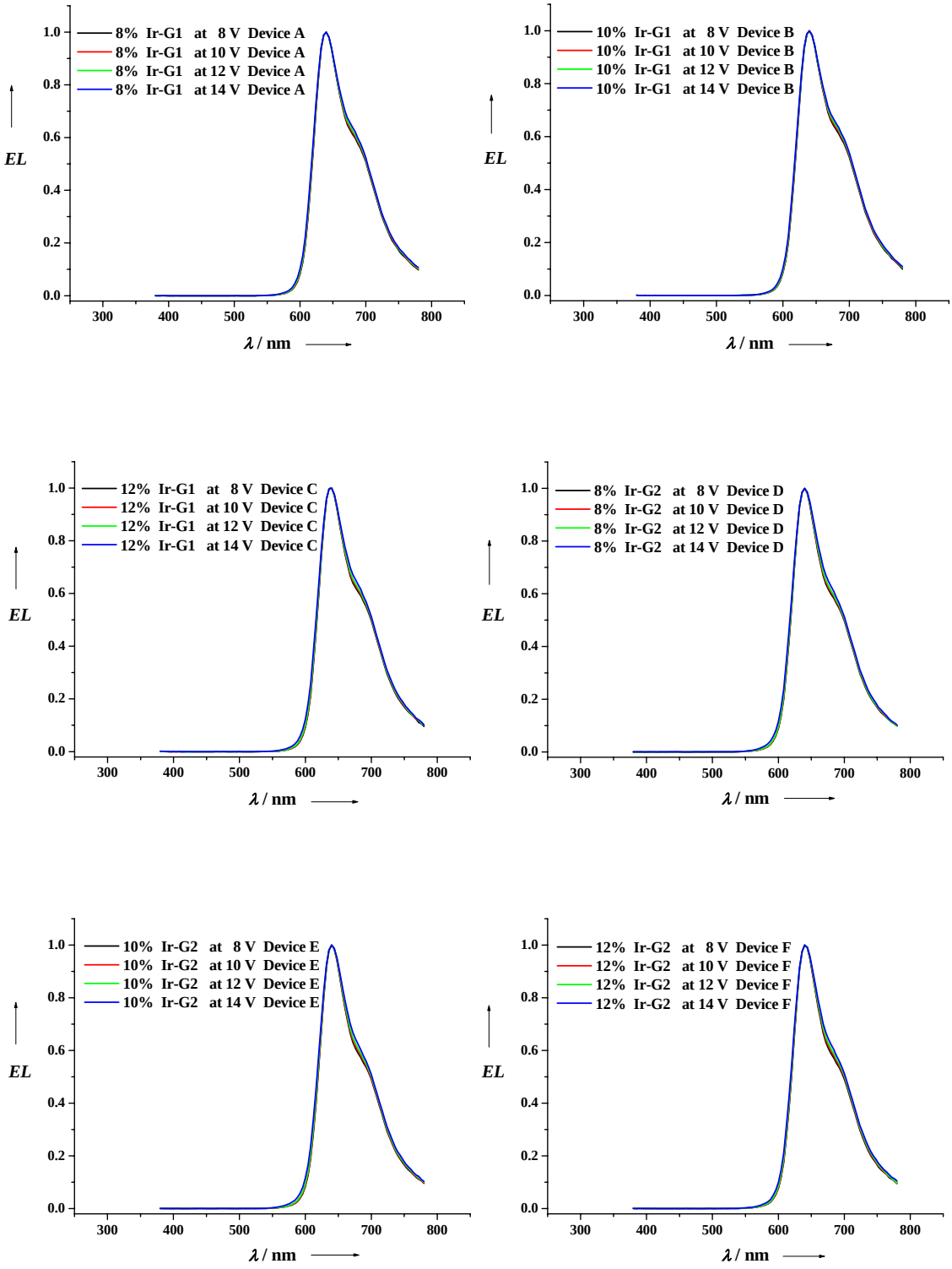

Figure S5. EL spectra for the devices with different doping levels of **Ir–G1** and **Ir–G2** at different applied voltages.

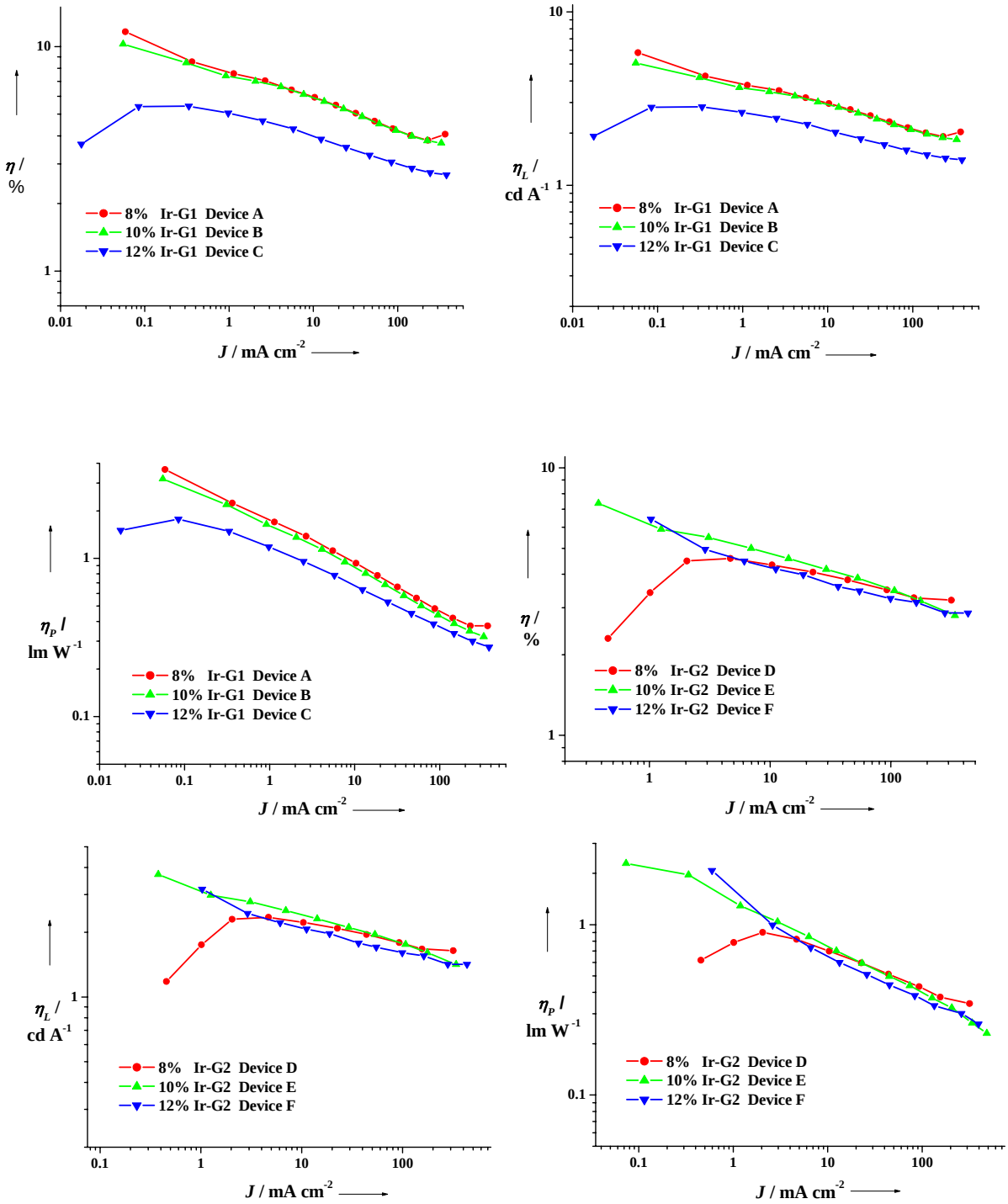

Figure S6. External quantum efficiency, luminance efficiency and power efficiency as a function of current density for solution-processed pure red phosphorescent OLEDs.

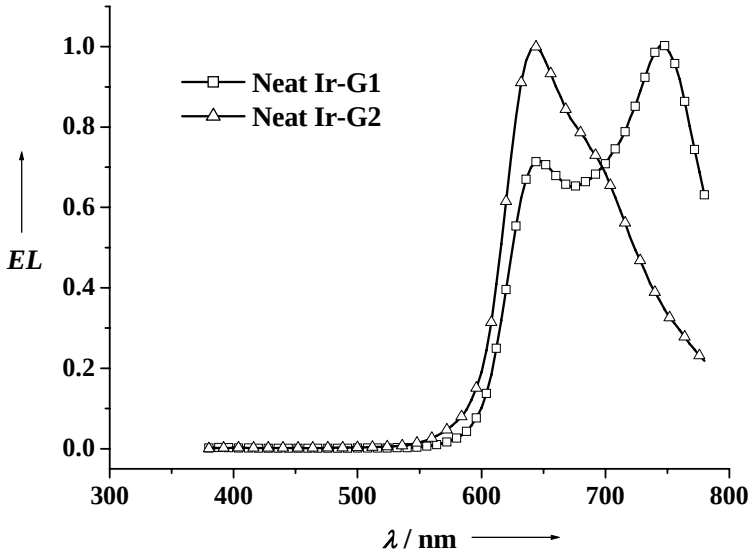

Figure S7. EL spectra for the devices with neat iridium dendrimers as the emitting layers (spin rate = 1500 rpm).